Journal of Applied Fluid Mechanics, Vol. 12, No. 1, pp. 271-280, 2019.
Available online at www.jafmonline.net, ISSN 1735-3572, EISSN 1735-3645.
DOI: 10.29252/jafm.75.253.29097

Double-Diffusive Bioconvection in a Suspension of Gyrotactic Microorganisms Saturated by Nanofluid

S. Saini† and Y. D. Sharma

Department of Mathematics, National Institute of Technology, Hamirpur, H.P., India-177005

†*Corresponding author email: shivani2291993@gmail.com*

(Received April 11, 2018; accepted September 2, 2018)

ABSTRACT

This paper focuses on analytical and numerical investigation of double-diffusive bioconvection in a porous media saturated by nanofluid using the modified mass flux condition. Normal mode technique is employed to solve the governing equations of the Brinkman-Darcy model. The Galerkin weighted residual method (single-term and six-term) is used to obtain numerical solution of the mathematical model. It is found that due to the presence of gyrotactic microorganisms, Rayleigh number is decreased substantially which shows that convection sets in earlier as compared to nanofluid without microorganisms and this destabilizing effect is more predominant for faster swimming microorganisms. modified Darcy number number, Soret parameter, and porosity postpone the onset of the bioconvection, whereas nanoparticle Rayleigh number, bioconvection Rayleigh number, nanoparticle Lewis number, Dufour parameter, Péclet number, and Lewis number pre-pone the onset of bioconvection under certain conditions.

Keywords: Bioconvection; Brownian motion; Gyrotactic microorganisms; Nanofluid; Porous medium; Thermophoresis.

1. INTRODUCTION

The bioconvection refers to a convection driven by the collective motion of a large number of self-propelled microorganisms which are heavier than the base fluid. The term "bioconvection" was first coined by Platt (1961). First mathematical model for negatively gravitactic bioconvection was developed by Childress *et al*. (1975). Mathematical models for the different species of microorganisms can be seen in papers (Pedley and Kessler 1987; Pedley *et al*. 1988; Bees and Hill 1997; Ghorai and Hill 1999; Metcalfe and Pedley 2001).

The term "nanofluid" was first coined by Chol (1995). Buongiorno (2006) developed a mathematical model for nanofluid and explored the various transport mechanisms of nanofluids. The growing volume of papers dedicated to the instability problems saturating nanofluid is well documented by (Tzou 2008; Nield and Kuznetsov 2009, 2010). Later, Chand and Rana (2012a) include the effect of rotation on nanofluid and found that rotation has a stabilizing effect. The onset of convection in a porous media saturated by nanofluid was presented by Chand and Rana (2012 b, 2012c). Nanofluids have many applications in microheat pipes, cooling, cancer therapy, micro-channel heat sinks, microreactors, heat transfer systems, aerospace tribology, polymer coatings, process industries, etc.

Nield and Kuznetsov (2014a, 2014b) suggested the more realistic flow on the boundaries. After that many research articles (Rana and Chand, 2015; Saini and Sharma 2017, 2018a, 2019) studied the onset of convection using the revised boundary conditions and found that revised boundary conditions(zero flux) have more destabilizing effect as compared to previous boundary conditions (constant nanoparticle fraction). Very recently, Yadav and Wang (2018) examined the convective heat transport in a non-Newtonian nanofluid.

Kuznetsov (2010, 2011) was the first who discovered the thermal instability in a nanofluid with gyrotactic microorganisms and reported that gyrotactic microorganisms always destabilize the system. Mixed convection flow in a nanofluid containing gyrotactic microorganisms was examined by Tham (2013). Shaw *et al*. (2014) analyzed the soret and MHD effect on bioconvection. The MHD bioconvection in the presence of chemical reaction was analyzed by Das *et al*. (2015). Mahdy (2016) investigated the boundary layer bioconvection along a vertical cone. Recently, Saini and Sharma (2018b, 2018c) presented the instability analysis of nanofluid bio-thermal convection with the effect of throughflow.

Pioneering work on double-diffusive convection in nanofluid has been examined by Nield and Kuznetsov (2011), and Yadav *et al*. (2012). Yadav *et al*. (2013) and Umavati *et al*. (2015) studied the effect of viscosity variation and thermal conductivity on double diffusive convection in rotating nanofluid and Maxwell nanofluid. Later, Yadav *et al*. (2016) revised their previous work (Yadav *et al*., 2013) by using more realistic boundary conditions. The readers are also referred to Akbar *et al*. (2017), Garaud (2018), and Reddy *et al*. (2018) for recent studies of double-diffusive convection.

The review of the literature reveals that the double-diffusive bioconvection in a nanofluid with modified boundary conditions has not been studied so far. In this article, the effect of double diffusion on bioconvection using the modified boundary conditions is investigated analytically and numerically. The effects of various controlling parameters of our interest on Rayleigh number are analyzed.

2. ANALYSIS

We consider an infinite horizontal layer of binary nanofluid with gyrotactic microorganisms in a porous medium confined between the boundaries z^* = 0 and z^* = H. The pore size is large compared to microorganisms and porous matrix does not absorb microorganisms. We use the Brinkman-Darcy model. Local thermal equilibrium and homogeneity in the porous medium are also assumed. We take temperatures T_h^* and T_c^* $(T_h^* > T_c^*)$, solute concentrations C_h^* and C_c^* $(C_c^* < C_h^*)$ respectively. The dimensionless governing equations are written below (Pedley and Hill 1987; Nield and Kuznetsov 2009; Kuznetsov 2010; Yadav *et al*. 2012).

$$\nabla.\mathbf{V}=0 \tag{1}$$

In Eq. (1), $\mathbf{V}$ is the dimensionless velocity.

$$\frac{D_a}{\varepsilon \Pr}\left(\frac{\partial \mathbf{V}}{\partial t}\right)=-\nabla p+\tilde{D}_a\nabla^2\mathbf{V}-\mathbf{V}-R_m\hat{\mathbf{k}}+R_aT\hat{\mathbf{k}} -R_n\phi\hat{\mathbf{k}}+\frac{R_s}{L_n}C\hat{\mathbf{k}}-\frac{R_b}{L_bV}n\hat{\mathbf{k}} \tag{2}$$

In Eq. (2), p is the pressure, t is the time, ϕ is the nanoparticles volume fraction, n is the microorganism concentration, ε is the porosity, $D_a=K/H^2$ is the Darcy number, $\Pr=\mu/\rho_f\alpha_m$ is the Prandtl number, $\tilde{D}_a=\bar{\mu}K/\mu H^2$ is the modified Darcy number, $R_n=\left((\rho_P-\rho)\phi_0^*\right)gKH/\alpha_m\mu$ is the nanoparticle Rayleigh number, $R_a=\rho\beta_TKHg(T_h^*-T_c^*)/\alpha_m\mu$ is the Rayleigh number, $R_m=(\phi_0^*\rho_P+\rho_f(1-\phi_0^*))gKH/\alpha_m\mu$ is the basic density Rayleigh number, $L_b=\alpha_m/D_m$ is the bioconvection Lewis number, $R_S=\rho\beta_C(C_h^*-C_c^*)gKH/\mu D_S$ is solutal Rayleigh number, $R_b=\Delta\rho gvKH/\mu D_m$ is the bioconvection Rayleigh number, $L_n=\alpha_m/D_S$ is Lewis number. Other parameters in Eq. (2) are as: $\bar{\mu}$ is effective viscosity, μ is the viscosity, ρ_p is nanoparticles density, ϕ_0 is reference volume fraction, K is the permeability, $\mathbf{g}$ is the gravity vector, ρ_f is the nanofluid density, $\Delta\rho=\rho_{cell}-\rho_f$ is the difference between cell density and a fluid density, β_c is the solutal coefficient, α_m is the thermal diffusivity of the porous media, D_m is the microorganism diffusivity, D_S is the solutal diffusivity.

$$\left(\frac{\partial}{\partial t}+\mathbf{V}.\nabla\right)T=\nabla^2T+\frac{N_B}{L_e}\nabla\phi.\nabla T+\frac{N_AN_B}{L_e}\nabla T.\nabla T +N_{TC}\nabla^2C \tag{3}$$

In Eq. (3), $L_e=\alpha_m/D_B$ is the nanofluid Lewis number, $N_B=\varepsilon\phi_0^*(\rho c)_p/(\rho c)_f$ is the particle density increment, $N_{TC}=D_{TC}(C_0^*-C_h^*)/\alpha_m(T_h^*-T_c^*)$ is the Dufour parameter, $N_A=(T_h^*-T_c^*)D_T/\phi_0^*T_c^*D_B$ is the modified diffusivity ratio. Other parameters in Eq. (3) are as follows: D_{TC} is the Dufour diffusivity, D_B is the Brownian diffusion coefficient, $(\rho c)_p$ is the heat capacity of the nanoparticles, D_T is the thermophoresis diffusivity, $(\rho c)_f$ is the heat capacity of the fluid.

$$\left(\frac{1}{\sigma}\frac{\partial}{\partial t}+\frac{1}{\varepsilon}\mathbf{V}.\nabla\right)C=\frac{1}{L_n}\nabla^2C+N_{CT}\nabla^2T \tag{4}$$

In Eq. (4), $N_{CT}=T_h^*-T_c^*)D_{CT}(/\alpha_m(C_h^*-C_c^*)$ is the Soret Parameter, D_{CT} is the soret diffusivity, σ is the thermal capacity ratio.

$$\frac{1}{\sigma}\frac{\partial\phi}{\partial t}+\frac{1}{\varepsilon}\mathbf{V}.\nabla\phi=\frac{1}{L_e}\nabla^2\phi+\frac{N_A}{L_e}\nabla^2T \tag{5}$$

$$\frac{1}{\sigma}\frac{\partial n}{\partial t}=-\nabla.\left(n\frac{1}{\varepsilon}\mathbf{V}+n\frac{Q}{L_b}\hat{\mathbf{p}}-\frac{1}{L_b}\nabla n\right) \tag{6}$$

In Eq. (6), $Q=W_cH/D_m$ is the Péclet number and $W_c\hat{\mathbf{p}}$ is average swimming velocity.

In component form, Eq. (2) can be written as:

$$\frac{D_a}{\varepsilon\Pr}\left(\frac{\partial u}{\partial t}\right)=-\frac{\partial p}{\partial x}+\tilde{D}_a\nabla^2u-u \tag{7a}$$

$$\frac{D_a}{\varepsilon\Pr}\left(\frac{\partial v}{\partial t}\right)=-\frac{\partial p}{\partial y}+\tilde{D}_a\nabla^2v-v \tag{7b}$$

$$\frac{D_a}{\varepsilon\Pr}\left(\frac{\partial w}{\partial t}\right)=-\frac{\partial p}{\partial z}+\tilde{D}_a\nabla^2w-w-R_m+R_aT -R_n\phi+\frac{R_s}{L_n}C-\frac{R_b}{L_bV}n \tag{7c}$$

Applying the operator $\partial/\partial x$ to the both sides of Eq. (7a) and $\partial/\partial y$ to the both sides of Eq. (7b), then adding and by using the Eq. (1), we get

$$-\frac{D_a}{\varepsilon \Pr}\frac{\partial}{\partial t}\left(\frac{\partial w}{\partial z}\right)=-\left(\frac{\partial^2 p}{\partial x^2}+\frac{\partial^2 p}{\partial y^2}\right)-\tilde{D}_a\nabla^2\left(\frac{\partial w}{\partial z}\right)+\frac{\partial w}{\partial z} \quad (8)$$

Now, applying the operator $\frac{\partial^2}{\partial x^2}+\frac{\partial^2}{\partial y^2}$ to the both sides of Eq. 7(c) and applying the operator $\frac{\partial}{\partial z}$ to the both sides of Eq. (8) then subtracting Eq. (8) from Eq. (7c) we get

$$\frac{D_a}{\varepsilon \Pr}\frac{\partial}{\partial t}\nabla^2 w-\tilde{D}_a\nabla^4 w+\nabla^2 w=R_a\nabla_H^2 T-R_n\nabla_H^2\phi+\left(\frac{R_s}{L_n}\right)\nabla_H^2 C-\frac{R_b}{L_b\nu}\nabla_H^2 n \quad (9)$$

where ∇_H^2 is the horizontal Laplacian operator in the 2-D plane.

In boundaries, we have taken the temperature and solute concentration to be constant, and in addition nanoparticle flux and microorganism's concentration flux are supposed to be zero on the boundaries. The boundary conditions are

$$\left.\begin{aligned}&\text{Rigid-rigid}: w=0,\frac{\partial w}{\partial z}=0, T=1,\ C=1,\\&\frac{\partial \phi}{\partial z}+N_A\frac{\partial T}{\partial z}=0, Qn=\frac{\partial n}{\partial z}, \qquad \text{at } z=0\\&w=0,\ \frac{\partial w}{\partial z}=0, T=0, C=0,\\&\frac{\partial \phi}{\partial z}+N_A\frac{\partial T}{\partial z}=0, Qn=\frac{\partial n}{\partial z}, \qquad \text{at } z=1\end{aligned}\right\} \quad (10a)$$

$$\left.\begin{aligned}&\text{Rigid-free}: w=0,\frac{\partial w}{\partial z}=0, T=1, C=1,\\&\frac{\partial \phi}{\partial z}+N_A\frac{\partial T}{\partial z}=0, Qn=\frac{\partial n}{\partial z} \qquad \text{at } z=0\\&w=0,\ \frac{\partial^2 w}{\partial z^2}=0, T=0,\ C=0,\\&\frac{\partial \phi}{\partial z}+N_A\frac{\partial T}{\partial z}=0, Qn=\frac{\partial n}{\partial z}, \qquad \text{at } z=1\end{aligned}\right\} \quad (10b)$$

The steady-state solutions of the Eqs. (3)-(6) are as

$$T_b(z)=1-z,\ \phi_b(z)=\phi_0+N_A z, C_b(z)=1-z,\ n_b(z)=\nu\ e^{Qz} \quad (11)$$

Here $\nu=\bar{n}Q/e^{Q}-1$ is the integration constant.

3. PERTURBED SOLUTIONS

For small perturbations on the basic solutions, we assume that

$$\mathbf{V}=\mathbf{V}', T=T_b+T', \phi=\phi_b+\phi', C=C_b+C', n=n_b+n' \quad (12)$$

Substituting Eq. (12) in Eqs. (3)-(6) and (9) and utilizing Eq. (11), we get

$$\frac{D_a}{\varepsilon \Pr}\frac{\partial}{\partial t}\nabla^2 w'-\tilde{D}_a\nabla^4 w'+\nabla^2 w'=R_a\nabla_H^2 T'-R_n\nabla_H^2\phi'+\left(\frac{R_s}{L_n}\right)\nabla_H^2 C'-\frac{R_b}{L_b\nu}\nabla_H^2 n' \quad (13)$$

$$\frac{\partial T'}{\partial t}-w'=\nabla^2 T'-\frac{N_B}{L_e}\left(N_A\frac{\partial T'}{\partial z}+\frac{\partial \phi'}{\partial z}\right)+N_{TC}\nabla^2 C' \quad (14)$$

$$\frac{1}{\sigma}\frac{\partial C'}{\partial t}-\frac{1}{\varepsilon}w'=\frac{1}{L_n}\nabla^2 C'+N_{CT}\nabla^2 T' \quad (15)$$

$$\frac{1}{\sigma}\frac{\partial \phi'}{\partial t}+\frac{N_A}{\varepsilon}w'=\frac{1}{L_e}\nabla^2\phi'+\frac{N_A}{L_e}\nabla^2 T' \quad (16)$$

$$\frac{1}{\sigma}\frac{\partial n'}{\partial t}=-\nabla.\left(n_b\left(\frac{\mathbf{V}'}{\varepsilon}+\frac{Q}{Lb}\hat{\mathbf{p}}\right)+n'\frac{Q}{Lb}\hat{\mathbf{k}}-\frac{1}{L_b}\nabla n'\right) \quad (17)$$

Applying the procedure outlined in Pedley *et al.* (1988) and Kuznetsov (2010) for average swimming direction vector, Eq. (17) can be expressed as

$$\frac{1}{\sigma}\frac{\partial n'}{\partial t}=-\frac{w'}{\varepsilon}\frac{\partial n_b}{\partial z}-\frac{Q}{L_b}\frac{\partial n'}{\partial z}-GQn_b((\alpha_0-1)\left(\frac{\partial^2 w'}{\partial x^2}+\frac{\partial^2 w'}{\partial y^2}\right)+(1+\alpha_0)\frac{\partial^2 w'}{\partial z^2}\Bigg)+\frac{1}{L_b}\nabla^2 n' \quad (18)$$

where G and α_0 are Gyrotactic number and measure of cell eccentricity respectively.

With

$$\left.\begin{aligned}&\text{Rigid-rigid}: w'=0,\frac{\partial w'}{\partial z}=0, C'=0,\ \frac{\partial n'}{\partial z}=n'Q,\\&\frac{\partial \phi'}{\partial z}+N_A\frac{\partial T'}{\partial z}=0, T'=0, \qquad \text{at } z=0,1\end{aligned}\right\} \quad (19a)$$

$$\left.\begin{aligned}&\text{Rigid-free}: w'=0,\frac{\partial w'}{\partial z}=0, C'=0,\frac{\partial n'}{\partial z}=n'Q,\\&\frac{\partial \phi'}{\partial z}+N_A\frac{\partial T'}{\partial z}=0, T'=0 \quad \text{at } z=0\\&w'=0,\frac{\partial^2 w'}{\partial z^2}=0, C'=0,\frac{\partial n'}{\partial z}=n'Q,\\&\frac{\partial \phi'}{\partial z}+N_A\frac{\partial T'}{\partial z}=0, T'=0 \qquad \text{at } z=1\end{aligned}\right\} \quad (19b)$$

Due to an absence of two opposite agencies which affect instability, oscillatory convection cannot occur. Assuming the normal modes as

$$[w',T',C',\phi',n']=[W(z),\Theta(z),\chi(z),\Phi(z),N(z)]f(x,y) \quad (20)$$

Here, $\frac{\partial^2 f}{\partial x^2}+\frac{\partial^2 f}{\partial y^2}=-a^2 f$

Substituting Eq. (20) in Eqs. (13)-(16),(18), we get

$$\left(\tilde{D}_a(D^2-a^2)^2-(D^2-a^2)\right)W-R_a a^2\Theta-\frac{R_S}{L_n}\alpha^2\chi+R_n a^2\Phi-\frac{R_b}{L_b\nu}a^2 N=0 \quad (21)$$

$$W+\left(D^2-\frac{N_A N_B}{L_e}D-a^2\right)\Theta-\frac{N_B}{L_e}D\Phi+N_{TC}(D^2-a^2)\chi=0 \quad (22)$$

$$\frac{N_A}{\varepsilon}W-\frac{N_A}{L_e}(D^2-a^2)\Theta-\left(\frac{1}{L_e}(D^2-a^2)\right)\Phi=0 \tag{23}$$

$$\frac{1}{\varepsilon}W+N_{CT}(D^2-a^2)\Theta+\left(\frac{1}{L_n}(D^2-a^2)\right)\chi=0 \tag{24}$$

$$\begin{aligned}&\frac{1}{L_b}a^2N+\frac{Q}{L_b}DN-\frac{1}{L_b}D^2N+e^{Qz}Qv\left(\frac{W}{\varepsilon}+Ga^2\right.\\&\left.(1-\alpha_0)W-G(1+\alpha_0)D^2W\right)=0\end{aligned} \tag{25}$$

where $D\equiv\dfrac{d}{dz}$

with

Rigid–rigid boundaries:

$$\begin{aligned}&W=0, DW=0,\ \chi=0,\ QN=DN,\\&D\Phi+N_AD\Theta=0, \Theta=0\ \text{ at } z=0, z=1\end{aligned} \tag{26a}$$

Rigid-free boundaries:

$$\begin{aligned}&W=0, DW=0, \chi=0, QN=DN,\\&D\Phi+N_AD\Theta=0\Theta=0\ \text{ at } z=0\\&W=0, D^2W=0, \chi=0, QN=DN,\\&D\Phi+N_AD\Theta=0, \Theta=0\ \text{ at } z=1\end{aligned} \tag{26b}$$

4. RIGID-RIGID BOUNDARIES

The differential Eqs. (21)-(25) are solved by using the Galerkin weighted residual method. Accordingly, Θ, Φ, χ, N and W are taken as

$$\begin{aligned}&\Theta=\sum_{i=1}^{N}P_i\Theta_i, \Phi=\sum_{i=1}^{N}Q_i\Phi_i, \chi=\sum_{i=1}^{N}R_i\chi_i,\\&N=\sum_{i=1}^{N}S_iN_i, W=\sum_{i=1}^{N}T_iW_i\end{aligned}$$

(27)

For Rigid-rigid boundaries, the base functions are chosen as

$$\begin{aligned}&\Theta_i=z^i(1-z), \Phi_i=-N_Az^i(1-z),\\&N_i=(i+2-Q)z^{i+1}+(Q-i-1)z^{i+2}\chi_i=z^i(1-z)\\&W_i=z^i(1-z)^2\quad i=1,2,\ldots,N\end{aligned} \tag{28}$$

where T_i, S_i, R_i, Q_i and P_i are constants.

4.1 Single-Term Galerkin Method

For single-term, we take N = 1. Substitute the Eqs. (27)-(28) in Eqs. (21)-(25), employing the standard method(Finalayson, 1972) gives the following eigen-value equation

$$\begin{aligned}&R_a=81a^2Q^4(10Q^4+a^2\tilde{\varsigma}^2)\{L_nN_AN_{TC}R_n+L_eR_n\\&(-1+L_nN_{TC}N_{CT})-R_s\}+\varepsilon\{Q^4(10Q^4+a^2\tilde{\lambda}^2)\\&\{-84(-1+\mathrm{L}_n\,N_{CT}N_{TC})\tilde{\alpha}(\tilde{D}_a\tilde{\beta}+\tilde{\gamma})-81a^2N_AR_n\\&+81a^2N_{CT}R_S\}+30240e^{Q/2}a^2(-1+\mathrm{L}_n\,N_{CT}N_{TC})\\&\tilde{\alpha}\tilde{\lambda}\{Q(\tilde{\delta}(1-Ga^2(-1+\alpha_0))-24Q^2G(1+\alpha_0))\cosh\left(\tfrac{Q}{2}\right)\\&+(-\tilde{\rho}(1-Ga^2(-1+\alpha_0))+4Q^2G\tilde{\eta}(1+\alpha_0))\\&\sinh\left(\tfrac{Q}{2}\right)\}\}R_b/81a^2Q^4(10Q^4+a^2\tilde{\varsigma}^2)(\varepsilon-L_nN_{TC})\end{aligned} \tag{29}$$

where

$$\begin{aligned}&\tilde{\alpha}=10+a^2, \tilde{\beta}=504+24a^2+a^4, \tilde{\gamma}=12+a^2,\\&\tilde{\delta}=66+Q^2, \tilde{\rho}=132+13Q^2, \tilde{\eta}=12+Q^2,\\&\tilde{\lambda}=-28+3Q^2, \tilde{\varsigma}=120-10Q^2+Q^4\end{aligned}$$

For the case when $R_b=0$, Eq. (29) reduces to

$$R_a=\frac{\begin{aligned}&27a^2\{L_nN_AN_{TC}R_n+L_eR_n(-1+L_nN_{TC}N_{CT})\\&-R_s\}+\varepsilon\{-28\tilde{\alpha}(\tilde{D}_a\tilde{\beta}+\tilde{\gamma})(-1+\mathrm{L}_n\,N_{CT}N_{TC})\\&-27a^2N_AR_n+27a^2N_{CT}R_S\}\end{aligned}}{27a^2(\varepsilon-L_nN_{TC})} \tag{30}$$

Same expression (Eq. (30)) for R_a was obtained by Yadav *et al*. (2012).

For the case when $N_{CT}\approx 0$ and $N_{TC}\approx 0$, Eqs. (29)-(30) reduce to

$$\begin{aligned}&R_a=\frac{28\tilde{\alpha}(\tilde{D}_a\tilde{\beta}+\tilde{\gamma})}{27a^2}-\left(\frac{L_e}{\varepsilon}+N_A\right)R_n-\frac{R_s}{\varepsilon}\\&\frac{\begin{aligned}&-(1120\tilde{\alpha}\tilde{\lambda}e^{Q/2}(Q(\tilde{\delta}(1-Ga^2(-1+\alpha_0))\\&-24Q^2G(1+\alpha_0))\cosh\left(\tfrac{Q}{2}\right)+(-\tilde{\rho}(1-Ga^2(-1+\alpha_0))\\&+4Q^2G\tilde{\eta}(1+\alpha_0))\sinh\left(\tfrac{Q}{2}\right))R_b)\end{aligned}}{3Q^4(10Q^4+a^2\tilde{\varsigma}^2)}\end{aligned} \tag{31}$$

$$R_a=\frac{28\tilde{\alpha}(\tilde{D}_a\tilde{\beta}+\tilde{\gamma})}{27a^2}-\left(\frac{L_e}{\varepsilon}+N_A\right)R_n-\frac{R_s}{\varepsilon} \tag{32}$$

For the case when $R_S=0$ and $R_n=0$, Eqs. (31)-(32) reduce to

$$\begin{aligned}&R_a=\frac{28\tilde{\alpha}(\tilde{D}_a\tilde{\beta}+\tilde{\gamma})}{27a^2}-(1120e^{Q/2}\tilde{\alpha}\tilde{\lambda}Q(\tilde{\delta}(1-Ga^2\\&(-1+\alpha_0))-24Q^2G(1+\alpha_0))\cosh\left(\tfrac{Q}{2}\right)+(-\tilde{\rho}(1-Ga^2\\&(-1+\alpha_0))+4Q^2G\tilde{\eta}(1+\alpha_0))\sinh\left(\tfrac{Q}{2}\right))\\&R_b/3Q^4(10Q^4+a^2\tilde{\varsigma}^2)\end{aligned} \tag{33}$$

$$R_a=\frac{28\tilde{\alpha}(D_a\tilde{\beta}+\tilde{\gamma})}{27a^2} \tag{34}$$

Same expression (Eq. (34)) for Rayleigh number was found by Kuznetsov and Nield (2010).

When $\tilde{D}_a=0$, Eq. (29) becomes

$$\begin{aligned}&R_a=81a^2Q^4(10Q^4+a^2\tilde{\varsigma}^2)\{L_nN_AN_{TC}R_n+L_eR_n\\&(-1+L_nN_{TC}N_{CT})-R_s\}+\varepsilon\{Q^4(10Q^4+a^2\tilde{\lambda}^2)\\&\{-84\tilde{\alpha}\tilde{\gamma}(-1+\mathrm{L}_n\,N_{CT}N_{TC})-81a^2N_AR_n+81a^2\\&N_{CT}R_s+30240e^{Q/2}a^2(-1+\mathrm{L}_n\,N_{CT}N_{TC})\tilde{\alpha}\tilde{\lambda}\\&\{Q(\tilde{\delta}(1-Ga^2(-1+\alpha_0))-24Q^2G(1+\alpha_0))\\&\cosh\left(\tfrac{Q}{2}\right)+(-\tilde{\rho}(1-Ga^2(-1+\alpha_0))+4Q^2G\tilde{\eta}(1+\\&\alpha_0))\sinh\left(\tfrac{Q}{2}\right)\}\}R_b/81a^2Q^4(10Q^4+a^2\tilde{\varsigma}^2)(\varepsilon-L_nN_{TC})\end{aligned} \tag{35}$$

In absence of microorganisms, R_a takes the minimum value at a = 3.31 and in this case when the value of $\tilde{D}_a$ is very large, it takes the minimum value at a = 3.117. These values exactly match with earlier reported work of Nield and Kuznetsov (2010).

To study the behavior of Péclet number Q and bioconvection Rayleigh number R_b we examine the $\frac{\partial R_a}{\partial Q}$ and $\frac{\partial R_a}{\partial R_b}$ analytically, we have

$$
\begin{aligned}
&560R_b\varepsilon\tilde{\alpha}(-1+L_nN_{TC}N_{CT})\Big(\tilde{\varsigma}Q\tilde{\lambda}\big(132-6\big(-1+24(1+\alpha_0)G\big)Q^2\big) \\
&-6a^2(-1+B)G(22+Q^2)+\tilde{\beta}+\big(-12\tilde{\varsigma}Q^2+\big(P(-8+Q) \\
&+40a^2Q^2-8(10+a^2)\big)Q^4\tilde{\lambda}\big)\tilde{\gamma})\cosh\left[\tfrac{Q}{2}\right]+(-8Q^2(10Q^2 \\
&+a^2(-5+Q^2))\tilde{\lambda}\tilde{\beta}+\tilde{\varsigma}(32(1+B)GQ^4\tilde{\lambda}+4Q^2((-13+(13a^2(-1 \\
&\underline{+\alpha_0)+48(1+\alpha_0))G)\tilde{\lambda}-3\tilde{\beta})-8\tilde{\lambda}\tilde{\beta}+Q\tilde{\lambda}\big(\tilde{\beta}+\tilde{\gamma}\big)))\sinh\left[\tfrac{Q}{2}\right]} \\
&\qquad\qquad 3e^{-Q/2}(\varepsilon-L_nN_{TC}N_{CT})\tilde{\varsigma}^2Q^5
\end{aligned}
$$

where

$$
\begin{aligned}
&\tilde{\alpha}=10+a^2,\tilde{\beta}=-132-13Q^2+G\Big(4(1+B)Q^2\big(12+Q^2\big)+a^2(-1+B)\big(132+13Q^2\big)\Big), \\
&\tilde{\gamma}=Q\Big(66+Q^2-G\Big(24(1+b)Q^2+a^2(-1+B)\big(66+Q^2\big)\Big)\Big) \\
&\tilde{\lambda}=-28+3Q_b^2,\ \tilde{\varsigma}=10Q_b^4+a^2\big(120-10Q_b^2+Q_b^4\big),
\end{aligned}
\tag{36}
$$

It is clear from the above expression that the behavior of Péclet number cannot be studied directly. To simplify the above expression α_0 is assumed to be zero, which corresponds to spherical microorganisms (Pedley and Kessler, 1987; Pedley *et al*., 1988) and we fixed the value of Gyrotactic number(G =0.03) and wave number(a= 3.12). Under these assumptions Eq. (36) becomes as follows:

For Q = 0.1(corresponds to slow swimmers)

$$\frac{\partial R_a}{\partial Q}=\frac{0.52\varepsilon(-1+L_nN_{CT}N_{TC})R_b}{\varepsilon-L_nN_{TC}} \tag{37a}$$

For Q =*1* (corresponds to intermediate swimmers)

$$\frac{\partial R_a}{\partial Q}=\frac{6.63\varepsilon(-1+L_nN_{CT}N_{TC})R_b}{\varepsilon-L_nN_{TC}} \tag{37b}$$

For Q = 10 (corresponds to fast swimmers)

$$\frac{\partial R_a}{\partial Q}=\frac{2.78\times10^4\varepsilon(-1+L_nN_{CT}N_{TC})R_b}{\varepsilon-L_nN_{TC}} \tag{37c}$$

From Eqs. (37a)-(37c), it is observed that Péclet number has a destabilizing effect if $1>L_nN_{TC}N_{CT}$ and $\varepsilon>L_nN_{TC}$. This effect is more predominant for faster swimmers. Using the above-stated assumptions, the expression for $\partial R_a/\partial R_b$ form Eq. (29) obtain as

$$\frac{\partial R_a}{\partial R_b}=\frac{k\varepsilon(-1+L_nN_{CT}N_{TC})}{\varepsilon-L_nN_{TC}} \tag{38}$$

where, k = 0.2(slow swimmers), 2.55(intermediate swimmers), 1.04×10^4 (fast swimmers). For all three values of Q, R_b has a destabilizing effect, if $1>L_nN_{TC}N_{CT}$ and $\varepsilon>L_nN_{TC}$.

4.2 Six-term Galerkin Method

In order to calculate the more accurate solution, six-term Galerkin method is utilized. For six-term Galerkin method, we take N = 6. Substitute the Eqs. (27)-(28) in Eqs. (21)-(25) and employing the standard Galerkin method, we get

$$\det\begin{bmatrix} A_1 & B_1 & C_1 & 0 & E_1 \\ A_2 & B_2 & 0 & 0 & E_2 \\ A_3 & 0 & C_3 & 0 & E_3 \\ 0 & 0 & 0 & D_4 & E_4 \\ A_5 & B_5 & C_5 & D_5 & E_5 \end{bmatrix}=0 \tag{39}$$

where,

$$B_1=\begin{bmatrix} -\langle\frac{N_B}{L_e}\Theta_1D\Phi_1\rangle & \cdots & -\langle\frac{N_B}{L_e}\Theta_1D\Phi_6\rangle \\ \vdots & \ddots & \vdots \\ -\langle\frac{N_B}{L_e}\Theta_6D\Phi_1\rangle & \cdots & -\langle\frac{N_B}{L_e}\Theta_6D\Phi_6\rangle \end{bmatrix},$$

$$C_1=\begin{bmatrix} \langle N_{TC}\left(D\Theta_1D\chi_1-a^2\Theta_1\chi_1\right)\rangle & \cdots & \langle N_{TC}\left(D\Theta_1D\chi_6-a^2\Theta_1\chi_6\right)\rangle \\ \vdots & \ddots & \vdots \\ \langle N_{TC}\left(D\Theta_1D\chi_6-a^2\Theta_1\chi_6\right)\rangle & \cdots & \langle N_{TC}\left(D\Theta_6D\chi_6-a^2\Theta_6\chi_6\right)\rangle \end{bmatrix},$$

$$E_1=\begin{bmatrix} \langle\Theta_1W_1\rangle & \cdots & \langle\Theta_1W_6\rangle \\ \vdots & \ddots & \vdots \\ \langle\Theta_6W_1\rangle & \cdots & \langle\Theta_6W_6\rangle \end{bmatrix},$$

$$A_2=\begin{bmatrix} \langle N_{CT}\left(D\chi_1D\Theta_1-a^2\chi_1\Theta_1\right)\rangle & \cdots & \langle N_{CT}\left(D\chi_1D\Theta_6-a^2\chi_1\Theta_6\right)\rangle \\ \vdots & \ddots & \vdots \\ \langle N_{CT}\left(D\chi_6D\Theta_1-a^2\chi_6\Theta_1\right)\rangle & \cdots & \langle N_{CT}\left(D\chi_6D\Theta_6-a^2\chi_6\Theta_6\right)\rangle \end{bmatrix},$$

$$B_2=\begin{bmatrix} \langle\frac{1}{L_n}\left(D\chi_1D\chi_1-a^2\chi_1\chi_1\right)\rangle & \cdots & \langle\frac{1}{L_n}\left(D\chi_1D\chi_6-a^2\chi_1\chi_6\right)\rangle \\ \vdots & \ddots & \vdots \\ \langle\frac{1}{L_n}\left(D\chi_6D\chi_1-a^2\chi_6\chi_1\right)\rangle & \cdots & \langle\frac{1}{L_n}\left(D\chi_6D\chi_6-a^2\chi_6\chi_6\right)\rangle \end{bmatrix},$$

$$E_2=\begin{bmatrix} \frac{1}{\varepsilon}\langle\chi_1W_1\rangle & \cdots & \frac{1}{\varepsilon}\langle\chi_1W_6\rangle \\ \vdots & \ddots & \vdots \\ \frac{1}{\varepsilon}\langle\chi_6W_1\rangle & \cdots & \frac{1}{\varepsilon}\langle\chi_6W_6\rangle \end{bmatrix}$$

$$A_3=\begin{bmatrix} \langle-\frac{N_A}{L_e}\left(D\Phi_1D\Theta_1-a^2\Phi_1\Theta_1\right)\rangle & \cdots & \langle-\frac{N_A}{L_e}\left(D\Phi_1D\Theta_6-a^2\Phi_1\Theta_6\right)\rangle \\ \vdots & \ddots & \vdots \\ \langle-\frac{N_A}{L_e}\left(D\Phi_6D\Theta_1-a^2\Phi_6\Theta_1\right)\rangle & \cdots & \langle-\frac{N_A}{L_e}\left(D\Phi_6D\Theta_6-a^2\Phi_6\Theta_6\right)\rangle \end{bmatrix},$$

$$C_3=\begin{bmatrix} \langle-\frac{1}{L_e}\left(D\Phi_1D\Phi_1-a^2\Phi_1\Phi_1\right)\rangle & \cdots & \langle-\frac{1}{L_e}\left(D\Phi_1D\Phi_6-a^2\Phi_1\Phi_6\right)\rangle \\ \vdots & \ddots & \vdots \\ \langle-\frac{1}{L_e}\left(D\Phi_6D\Phi_1-a^2\Phi_6\Phi_1\right)\rangle & \cdots & \langle-\frac{1}{L_e}\left(D\Phi_6D\Phi_6-a^2\Phi_6\Phi_6\right)\rangle \end{bmatrix},$$

$$A_5=\begin{bmatrix} \langle-R_aa^2W_1\Theta_1\rangle & \cdots & \langle-R_aa^2W_1\Theta_6\rangle \\ \vdots & \ddots & \vdots \\ \langle-R_aa^2W_6\Theta_1\rangle & \cdots & \langle-R_aa^2W_6\Theta_6\rangle \end{bmatrix},$$

$$B_5=\begin{bmatrix} \langle-\frac{R_s}{L_n}a^2W_1\chi_1\rangle & \cdots & \langle-\frac{R_s}{L_n}a^2W_1\chi_6\rangle \\ \vdots & \ddots & \vdots \\ \langle-\frac{R_s}{L_n}a^2W_6\chi_1\rangle & \cdots & \langle-\frac{R_s}{L_n}a^2W_6\chi_6\rangle \end{bmatrix},$$

$$C_5=\begin{bmatrix} <R_n a^2 W_1 \Phi_1> & \cdots & <R_n a^2 W_1 \Phi_6> \\ \vdots & \ddots & \vdots \\ <R_n a^2 W_6 \Phi_1> & \cdots & <R_n a^2 W_6 \Phi_6> \end{bmatrix},$$

$$D_5=\begin{bmatrix} <\frac{R_b}{L_b \nu} a^2 W_1 N_1> & \cdots & <\frac{R_b}{L_b \nu} a^2 W_1 N_6> \\ \vdots & \ddots & \vdots \\ <\frac{R_b}{L_b \nu} a^2 W_6 N_1> & \cdots & <\frac{R_b}{L_b \nu} a^2 W_6 N_6> \end{bmatrix},$$

$$A_1=<D\Theta_i D\Theta_j-\frac{N_A N_B}{L_e}\Theta_i\Theta_j-a^2\Theta_i\Theta_j>,$$

$$C_4=<-\frac{1}{L_b}(DN_iDN_j-QN_iN_j)-a^2N_iN_j>$$

$$D_4=<e^{Qz}Q\nu((1+Ga^2)N_iW_j-GN_iD^2W_j)>$$

$$E_5=<\tilde{D}_a(D^2W_iD^2W_j-2a^2DW_iDW_j+a^4W_iW_j)-(DW_iDW_j-a^2W_iW_j)>$$

$$\text{Here,} <\bullet>=\int_0^1(\bullet)dz,\quad i,j=1,2,3...,6$$

In Eq. (43), the Rayleigh number is a function of $L_e, L_n, Q, N_{TC}, N_{CT}, a, \varepsilon, N_A, N_B, R_b, R_n, R_S$ and $\tilde{D}_a$.

5. RIGID-FREE BOUNDARIES

For rigid-free boundaries, the minimal polynomials are chosen as

$$\Theta_1=z-z^2, \Phi_1=-N_A(z-z^2), \chi_1=z-z^2,$$
$$N_1=2+Q(2z-1)=Q^2(z^2-z), W_1=z^2(3-2z)(1-z) \quad (40)$$

This produces the following expression for R_a

$$\begin{aligned}R_a&=85683a^2Q^4(10Q^4+a^2\tilde{\varsigma}^2)\{L_nN_AN_{TC}R_n\\&+L_eR_n(-1+L_nN_{TC}N_{CT})-R_s\}+\varepsilon\{Q^4(10Q^4+a^2\tilde{\lambda}^2)\\&\{-4732\tilde{\alpha}(\tilde{D}_a\tilde{\beta}+\tilde{\gamma})(-1+L_nN_{CT}N_{TC})-85683a^2N_A\\&R_n+85683a^2N_{CT}R_S\}+212940e^{Q/2}a^2(-1+L_n\\&N_{CT}N_{TC})\tilde{\alpha}\tilde{\lambda}\{Q(\tilde{\delta}-G(a^2\tilde{\delta}(-1+\alpha_0-24Q^2(16+Q)\\&(1+\alpha_0)))\cosh\left(\tfrac{Q}{2}\right)+(-\tilde{\rho}+G(a^2\tilde{\rho}(-1+\alpha_0)+12Q^2\\&\tilde{\eta}(1+\alpha_0)))\sinh\left(\tfrac{Q}{2}\right)\}\}R_b/85683a^2Q^4(10Q^4\\&+a^2\tilde{\varsigma}^2)(\varepsilon-L_nN_{TC})\end{aligned}\quad (41)$$

Where,

$$\tilde{\alpha}=10+a^2, \tilde{\beta}=4536+432a^2+19a^4, \tilde{\gamma}=216+19a^2,$$
$$\tilde{\varsigma}=120-10Q^2+Q^4, \tilde{\delta}=1056+84Q+8Q^2+Q^3,$$
$$\tilde{\rho}=2112+168Q+192Q^2+16Q^3+Q^4, \tilde{\eta}=64+$$
$$4Q+5Q^2, \tilde{\lambda}=-126-7Q+13Q^2$$

In the case of no microorganisms, Eq. (41) reduces to

$$\begin{aligned}R_a&=507a^2\{L_nN_AN_{TC}R_n+L_eR_n(-1+L_nN_{TC}N_{CT})\\&-R_s\}+\varepsilon\{-28\tilde{\alpha}(\tilde{D}_a\tilde{\beta}+\tilde{\gamma})(-1+L_nN_{CT}N_{TC})\\&-27a^2N_AR_n+27a^2N_{CT}R_S\}/507a^2(\varepsilon-L_nN_{TC})\end{aligned}\quad (42)$$

This expression is the same as obtained by Yadav *et al*. (2012).

When $N_{CT}\approx 0$ and $N_{TC}\approx 0$ are insignificant then Eq. (41) and Eq. (42) reduce to

$$\begin{aligned}R_a&=\frac{28\tilde{\alpha}(\tilde{D}_a\tilde{\beta}+\tilde{\gamma})}{507a^2}-\left(\frac{L_e}{\varepsilon}+N_A\right)R_n-\frac{R_s}{\varepsilon}-420e^{Q/2}\\&\tilde{\alpha}\tilde{\lambda}[Q(\tilde{\delta}-G(a^2\tilde{\delta}(-1+\alpha_0)-24Q^2(16+Q)(1+\alpha_0))\\&)\cosh\left(\tfrac{Q}{2}\right)+(-\tilde{\rho}+G(a^2\tilde{\rho}(-1+\alpha_0)+12Q^2\tilde{\eta}(1+\alpha_0)\\&))\sinh\left(\tfrac{Q}{2}\right)]R_b/169Q^4(10Q^4+a^2\tilde{\varsigma}^2)\end{aligned}\quad (43)$$

$$R_a=\frac{28\tilde{\alpha}(\tilde{D}_a\tilde{\beta}+\tilde{\gamma})}{507a^2}-\left(\frac{L_e}{\varepsilon}+N_A\right)R_n-\frac{R_s}{\varepsilon}\quad (44)$$

In the absence of nanoparticles and solute ($R_n=0, N_{CT}=0, N_{TC}=0, R_S=0$), Eq. (43) reduces to

$$\begin{aligned}R_a&=\frac{28\tilde{\alpha}(\tilde{D}_a\tilde{\beta}+\tilde{\gamma})}{507a^2}-420e^{Q/2}\tilde{\alpha}\tilde{\lambda}[Q(\tilde{\delta}-G(a^2\tilde{\delta}(-1\\&+\alpha_0)-24Q^2(16+Q)(1+\alpha_0)))\cosh\left(\tfrac{Q}{2}\right)+(-\tilde{\rho}+\\&G(a^2\tilde{\rho}(-1+\alpha_0)+12Q^2\tilde{\eta}(1+\alpha_0)))\sinh\left(\tfrac{Q}{2}\right)]\\&R_b/169Q^4(10Q^4+a^2\tilde{\varsigma}^2)\end{aligned}\quad (45)$$

In the absence of microorganisms, Eq. (45) becomes

$$R_a=\frac{28\tilde{\alpha}(\tilde{D}_a\tilde{\beta}+\tilde{\gamma})}{507a^2}\quad (46)$$

The same expression for regular fluid was also obtained by Yadav *et al*.(2012).

For the case when $\tilde{D}_a=0$, Eq. (42) becomes

$$\begin{aligned}R_a&=85683a^2Q^4(10Q^4+a^2\tilde{\varsigma}^2)\{L_nN_AN_{TC}R_n+L_eR_n\\&(-1+L_nN_{TC}N_{CT})-R_s\}+\varepsilon\{Q^4(10Q^4+a^2\tilde{\lambda}^2)\\&\{-4732\tilde{\alpha}\tilde{\gamma}(-1+L_nN_{CT}N_{TC})-85683a^2N_AR_n\\&+85683a^2N_{CT}R_S\}+212940e^{Q/2}a^2\\&(-1+L_nN_{CT}N_{TC})\tilde{\alpha}\tilde{\lambda}\{Q(\tilde{\delta}-G(a^2\tilde{\delta}(-1+\alpha_0)\\&-24Q^2(16+Q)(1+\alpha_0)))\cosh\left(\frac{Q}{2}\right)+(-\tilde{\rho}+G(a^2\tilde{\rho}\\&(-1+\alpha_0)+12Q^2\tilde{\eta}(1+\alpha_0)))\sinh\left(\tfrac{Q}{2}\right)\}\}R_b/85683a^2\end{aligned}\quad (47)$$

In absence of microorganisms, it takes the minimum at a = 3.27 and minimum value is 48.01 which are same as obtained by Kuznetsov and Nield (2010).

6. RESULTS AND DISCUSSION

The values of dimensionless parameters are taken from (Pedley and Kessler 1988; Nield and Kuznetsov 2009; Kuznetsov 2010; Yadav *et al*., 2012) as:

$$\begin{aligned}&N_A=5, N_B=0.0075, L_b=4, L_e=5000, \alpha_0=0.31, Q=4,\\&\nu=3.7\times10^{-5}, G=0.03, R_b=3.0, \Pr=5, N_{TC}=0.03,\\&N_{CT}=2, L_n=2R_n=0.1, R_s=500, \varepsilon=0.7, \tilde{D}_a=0.8.\end{aligned}\quad (46)$$

The effect of R_s on Rayleigh number is discussed in Fig. 1. It is observed that as the value of R_s increases, the Rayleigh number also increases. This shows that R_s has a stabilizing effect.

From Fig. 2, it is observed that the nanoparticle

Rayleigh number accelerates the bioconvection. This result is expected from a physical point of view also because an increase in a volumetric fraction increases the Brownian motion of nanoparticles which produce a destabilizing effect.

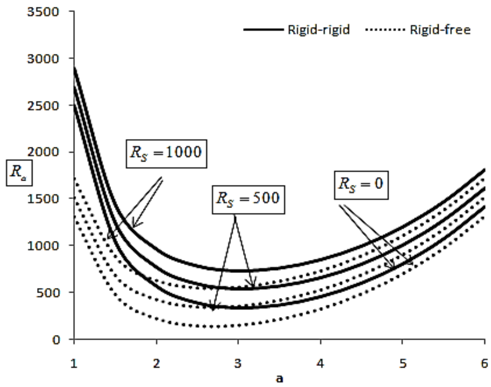

Fig. 1. Plots of $\mathbf{R_a}$ with *a* for various values of $\mathbf{R_s}$.

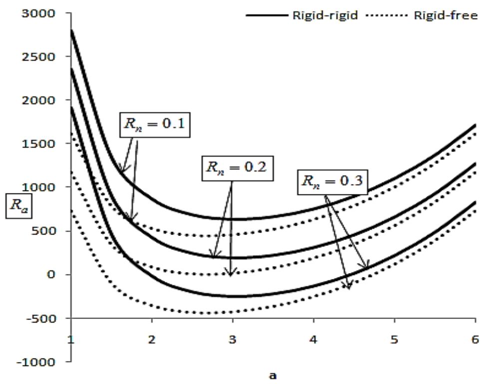

Fig. 2. Plots of $\mathbf{R_a}$ with *a* for various values of $\mathbf{R_n}$.

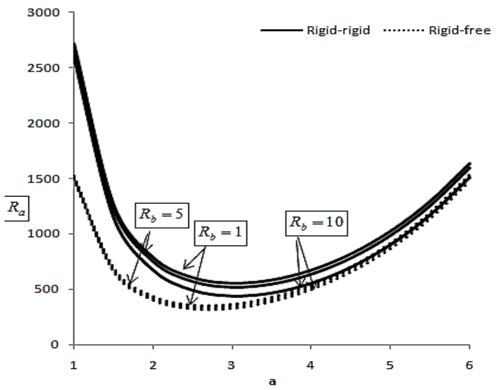

Fig. 3. Plots of $\mathbf{R_a}$ with *a* for various values of $\mathbf{R_b}$.

Figure 3 includes the curves against the variation of R_b . It is noticed that an increase in the value of R_b enhances the concentration of gyrotactic microorganisms at the top and develops top-heavy density stratification, resulting from that the instability sets in an earlier stage.

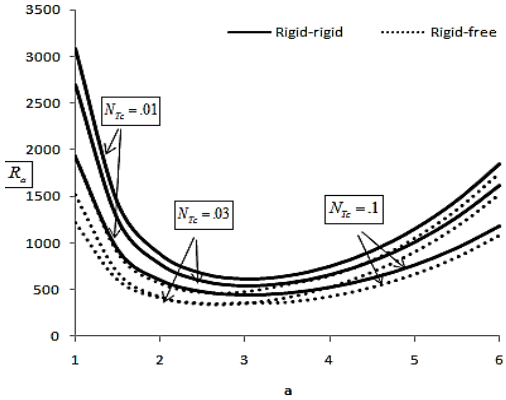

Fig. 4.Plots of $\mathbf{R_a}$ with *a* for various values of $\mathbf{N_{TC}}$.

Figures 4 and 5 summarize the variation of R_a for Soret and Dufour parameters. From Fig. 4, it is noted that R_a decreases with increasing value of N_{TC} . From Fig. 5, it is seen that as the value of

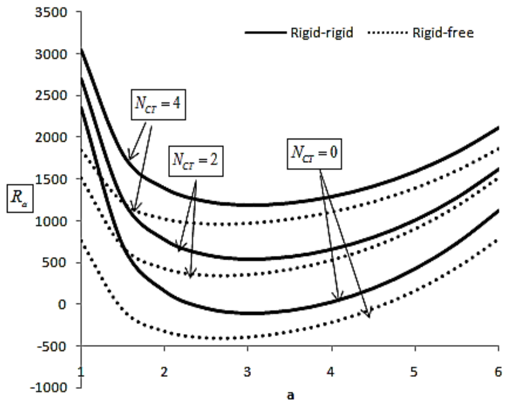

Fig. 5. Plots of $\mathbf{R_a}$ with *a* for various values of $\mathbf{N_{CT}}$.

N_{CT} increases the Rayleigh number increases. Thus it can be concluded that Soret parameter has a stabilizing effect whereas Dufour parameter has a destabilizing effect.

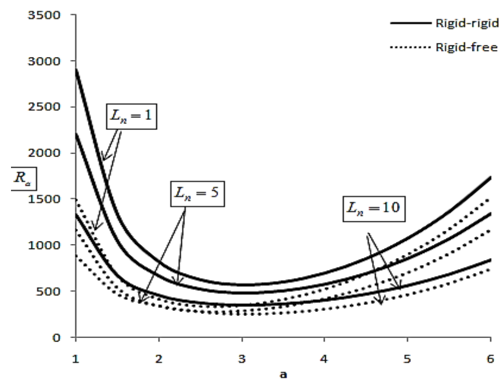

Fig. 6. Plots of $\mathbf{R_a}$ with *a* for various values of $\mathbf{L_n}$.

From Fig. 6, it is observed that Lewis number has a destabilising effect. By definition, Lewis number is inversely proportional to D_s and is directly proportional to α_m. Therefore, it can be concluded that an increase in solutal diffusivity (D_s) delays the bioconvection.

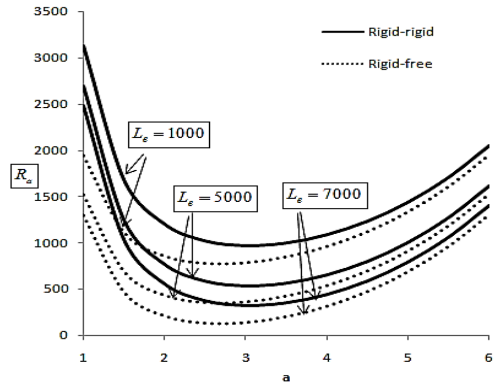

Fig. 7. Plots of $\mathbf{R_a}$ with *a* for various values of $\mathbf{L_e}$.

The effect of L_e on R_a is shown in Fig. 7. From Fig. 7, it is noticed that Rayleigh number decreases with increasing value of nanoparticle Lewis number. An increase in L_e reduces the mass diffusivity of the nanofluid which increases the nanoparticle volume fraction and subsequently increases the amount of heat transfer.

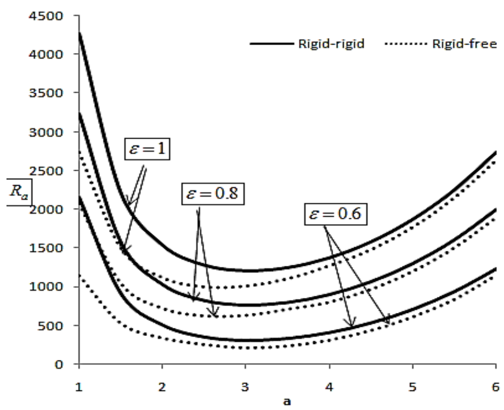

Fig. 8. Plots of $\mathbf{R_a}$ with a for various values of $\mathbf{L_e}$.

Figure 8 displays the effect of the porosity. We notice that the Rayleigh number exhibits a significant increase when porosity ε increases. Thus porosity has a stabilizing effect.

From Fig. 9 it is clear that $\tilde{D}a$ stabilizes the system, which we would physically expect because an increase in modified Darcy number results an increase in the effective viscosity, which slows down the forming of bioconvection pattern. Therefore modified Darcy number hinders the development of bioconvection.

Figure 10 displays the plot of Rayleigh number R_a for Q . It is found that Q accelerates the convection. Faster swimmers produce stronger disturbances, which promote the development of bioconvection and resulting in lowering the Rayleigh number for the larger value of Q.

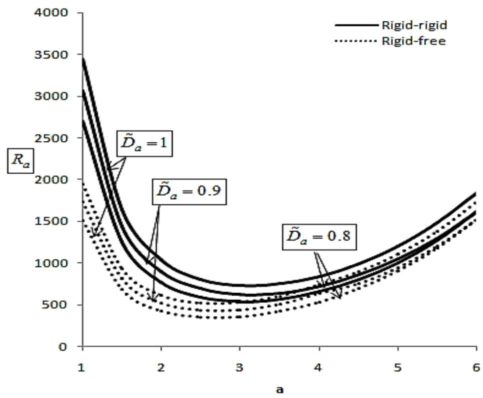

Fig. 9. Plots of $\mathbf{R_a}$ with a for various values of $\tilde{\mathbf{D}}_\mathbf{a}$.

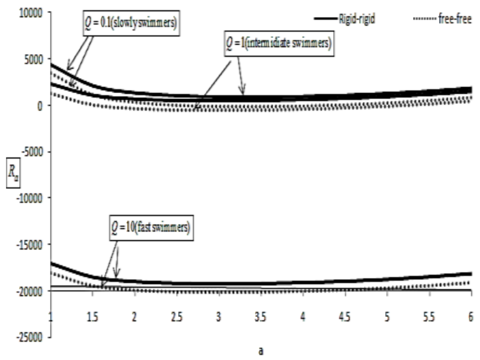

Fig. 10. Plots of $\mathbf{R_a}$ with a for various values of *Q*.

Table 1 Comparative results of $\mathbf{R_a}$ for various values of $\tilde{\mathbf{D}}_\mathbf{a}$ with Guo and Kaloni (1995) in a regular fluid for the (a) single-term (b) six-term

$\tilde{D}_a$	Guo and Kaloni (1995)	single-term		six-term	
	$R_{a,c}$	$R_{a,c}$	Error (%)	$R_{a,c}$	Error (%)
0.01	60.35	63.09	4.33	60.39	.045
0.1	215.06	220.6	2.54	215.08	.009
1	1752.20	1795.67	2.42	1752.87	.038
∞	1707.70	1749.98	2.42	1707.76	.004

Table 1 displays a comparison between the values of the critical Rayleigh number obtained by six-term and single-term Galerkin method with earlier reported work of Guo and Kaloni (1995) for regular fluid. It is observed that the higher order Galerkin method significantly improves the results and reduces the error.

7. CONCLUSIONS

The double-diffusive bioconvection in a suspension of gyrotactic microorganisms is studied for Rigid-free and Rigid-rigid boundaries. On using the six-term Galerkin weighted residual method, reasonably accurate solutions are obtained and it is found that Rayleigh number is dependent on modified particle density increment while in single-term method Rayleigh number is not affected by modified particle density increment. Rigid-free boundaries produce more unsteady bioconvection pattern as compared to Rigid-rigid boundaries. To study the behavior of Péclet number and bioconvection Rayleigh number, complex expressions are simplified by valid assumptions. Faster swimmers produce stronger disturbance as compared to slow swimmers, it thus facilitates the development of bioconvection resulting in a lower Rayleigh number at a larger value of Péclet number. The much lower Rayleigh number shows that the convection sets in earlier as compared to nanofluid without microorganisms. Modified Darcy number, Soret parameter, and porosity delay the bioconvection whereas bioconvection Rayleigh number, Lewis number, Dufour parameter, nanoparticle Lewis number, and nanoparticle Rayleigh number accelerate the bioconvection under the certain conditions. Solute delays the onset of bioconvection in the presence of Soret and Dufour parameter while in absence of Soret and Dufour parameter it accelerates the bioconvection.

REFERENCES

Akbar, N. S., C. M. Khalique and Z. H. Khan (2017). Double diffusion effects on magnetohydrodynamic non-Newtonian fluid nanoparticles. *Journal of Computational and Theoretical Nanoscience* 14(1), 694–703.

Bees, M. A. and N. A. Hill (1997). Wavelengths of bioconvection patterns. *The Journal of Experimental Biology* 200, 1515–1526.

Buongiorno, J. (2006). Convective transport in nanofluids. *Journal of Heat Transfer* 128(3), 240–250.

Chand, R. and G. C. Rana (2012a). On the onset of thermal convection in rotating nanofluid layer saturating a Darcy–Brinkman porous medium. *International Journal of Heat and Mass Transfer* 55, 5417–5424.

Chand, R. and G. C. Rana (2012b). Thermal Instability of Rivlin–Ericksen elastico-viscous nanofluid saturated by a porous medium. *Journal of Fluids Engineering* 134(12), 121203.

Chand, R. and G. C. Rana (2012c). Oscillating convection of nanofluid in porous medium. *Transport in Porous Media* 95(2), 269–284.

Childress, S., M. Levandowsky and E. A. Spiegel (1975). Pattern formation in a suspension of swimming micro-organisms: equations and stability theory. *Journal of Fluid Mechanics* 69(3), 591–613.

Chol, S. U. S. (1995). Enhancing thermal conductivity of fluids with nanoparticles. *ASME-Publications-Fed* 231, 99–106.

Das, K., P. R. Duari and P. K. Kundu (2015). Nanofluid bioconvection in presence of gyrotactic microorganisms and chemical reaction in a porous medium. *Journal of Mechanical Science and Technology* 29(11), 4841-4849.

Finalayson, B. A. (1972).*The method of weighted residuals and variational principles*. Academic press, New York.

Garaud, P. (2018). Double-diffusive convection at low Prandtl number. *Annual Review of Fluid Mechanics* 50, 275–298.

Ghorai, S. and N. A. Hill (1999). Development and stability of gyrotactic plumes in bioconvection. *Journal of Fluid Mechanics* 400, 1–31.

Guo, J. and P. N. Kaloni (1995). Double-Diffusive Convection in a Porous Medium, Nonlinear Stability, and the Brinkman Effect. *Studies in Applied Mathematics* 94(3), 341–358.

Kuznetsov, A. V. (2010). The onset of nanofluid bioconvection in a suspension containing both nanoparticles and gyrotactic microorganisms. *International Communications in Heat and Mass Transfer* 37(10), 1421–1425.

Kuznetsov, A. V. (2011). Non-oscillatory and oscillatory nanofluid bio-thermal convection in a horizontal layer of finite depth. *European Journal of Mechanics-B/Fluids* 30(2), 156–165.

Kuznetsov, A. V. and D. A. Nield (2010). Thermal instability in a porous medium layer saturated by a nanofluid: Brinkman model. *Transport in Porous Media* 81(3), 409–422.

Mahdy, A. (2016). Natural convection boundary layer flow due to gyrotactic microorganisms about a vertical cone in porous media saturated by a nanofluid. *Journal of the Brazilian Society of Mechanical Sciences and Engineering* 38(1), 67–76.

Metcalfe, A. M. and T. J. Pedley (2001). Falling plumes in bacterial bioconvection. *Journal of Fluid Mechanics* 445, 121–149.

Nield, D. A. and A. V. Kuznetsov (2011). The onset of double-diffusive convection in a nanofluid layer. *International Journal of Heat and Fluid Flow 32*(4), 771-776.

Nield, D. A. and A. V. Kuznetsov (2009). Thermal instability in a porous medium layer saturated by a nanofluid. *International Journal of Heat and Mass Transfer* 52(25), 5796–5801.

Nield, D. A. and A. V. Kuznetsov (2010). The onset of convection in a horizontal nanofluid layer of finite depth. *European Journal of Mechanics-B/Fluids 29*(3), 217–223.

Nield, D. A. and A. V. Kuznetsov (2014a). Thermal instability in a porous medium layer saturated by a nanofluid: A revised model. *International Journal of Heat and Mass Transfer* 68, 211–214.

Nield, D. A. and A. V. Kuznetsov (2014b). The onset of convection in a horizontal nanofluid layer of finite depth: A revised model. *International Journal of Heat and Mass Transfer 77*, 915–918.

Pedley, T. J. and J. O. Kessler (1987). The orientation of spheroidal microorganisms swimming in a flow field. *Proceedings of the Royal Society of London B: Biological Sciences 231*(1262), 47–70.

Pedley, T. J., N. A. Hill and J. O. Kessler (1988). The growth of bioconvection patterns in a uniform suspension of gyrotactic micro-organisms. *Journal of Fluid Mechanics 195*(1), 223.

Platt, J. R. (1961). "Bioconvection Patterns" in Cultures of Free-Swimming Organisms. *Science 133*(3466), 1766–1767.

Rana, G. C. and R. Chand (2015). Onset of thermal convection in a rotating nanofluid layer saturating a Darcy-Brinkman porous medium: a more realistic model. *Journal of Porous Media 18*(6), 629-635.

Reddy, M. G., N. Sandeep, S. Saleem and M. T. Mustafa (2018). Magnetohydrodynamic Bio-Convection Flow of Oldroyd-B Nanofluid Past a Melting Sheet with Cross Diffusion. *Journal of Computational and Theoretical Nanoscience 15*(4), 1348–1359.

Saini, S. and Y. D. Shamra (2017). The effect of vertical throughflow in Rivlin–Ericksen elastico-viscous nanofluid in a non-Darcy porous medium. *Nanosystems: physics, chemistry, mathematics 8*(5), 606–612.

Saini, S. and Y. D. Shamra (2018a). Thermal Convection in a Rectangular Box Saturated by Nanofluid with Convective Boundary Condition. *International journal of nanoparticles.* 10(4), 275-285.

Saini, S. and Y. D. Sharma (2018b). A Bio-Thermal Convection in Water-Based Nanofluid Containing Gyrotactic Microorganisms: Effect of Vertical Throughflow. *Journal of Applied Fluid Mechanics 11*(4).

Saini, S. and Y. D. Sharma (2018c). Numerical study of nanofluid thermo-bioconvection containing gravitactic microorganisms in porous media: Effect of vertical throughflow. *Advanced Powder Technology*. 29(11), 2725-2732.

Saini, S. and Y. D. Sharma (2019). Linear Instability of the Throughflow in a Rectangular Box Saturated by a Nanofluid. *Journal of Applied Fluid Mechanics*, 12(3) (In press)

Shaw, S., P. Sibanda, A. Sutradhar and P. Murthy (2014). Magnetohydrodynamics and soret effects on bioconvection in a porous medium saturated with a nanofluid containing gyrotactic microorganisms. *Journal of Heat Transfer* 136(5), 52601.

Tham, L., R. Nazar and I. Pop (2013). Mixed convection flow over a solid sphere embedded in a porous medium filled by a nanofluid containing gyrotactic microorganisms. *International Journal of Heat and Mass Transfer* 62, 647–660.

Tzou, D. Y. (2008). Thermal instability of nanofluids in natural convection. *International Journal of Heat and Mass Transfer 51*(11), 2967–2979.

Umavathi, J. C., D. Yadav, M. B. Mohite (2015). Linear and nonlinear stability analyses of double-diffusive convection in a porous medium layer saturated in a Maxwell nanofluid with variable viscosity and conductivity. *Elixir Mech Eng 79*, 30407-26.

Yadav, D. and J. Wang (2018). Convective Heat Transport in a Heat Generating Porous Layer Saturated by a Non-Newtonian Nanofluid. *Heat Transfer Engineering*, 1-20.

Yadav, D., G. S. Agrawal and R. Bhargava (2012). The onset of convection in a binary nanofluid saturated porous layer. *International Journal of Theoretical and Applied Multiscale Mechanics 2*(3), 198–224.

Yadav, D., G. S. Agrawal and R. Bhargava (2013). Onset of double-diffusive nanofluid convection in a layer of saturated porous medium with thermal conductivity and viscosity variation. *Journal of Porous Media 16*(2).

Yadav, D., R. A. Mohamed, H. H. Cho and J. Lee (2016). Effect of Hall Current on the Onset of MHD Convection in a Porous Medium Layer Saturated by a Nanofluid. *Journal of Applied Fluid Mechanics 9*(5), 2379-2389.